

## Targeted Drug Delivery Using Smart Nanoparticles

**Running Title:** Nanoparticles in Precision Drug Delivery

Mohammad Javad Sohrabi<sup>1\*</sup>, Parisa Miralinaghi<sup>2</sup>, Mohammad Reza Sohrabi Renani<sup>3</sup>, Fatemeh Gharishvandi<sup>4</sup>

<sup>1</sup>Department of pharmacology, Faculty of pharmaceutical, Damghan Islamic Azad University, Damghan, Iran.

<sup>2</sup>Department of Medicinal chemistry, Faculty of pharmaceutical, Damghan Islamic Azad University, Damghan, Iran.

<sup>3</sup>Department of medicine, Faculty of medicine, Guilan University of Medical Sciences, Rasht, Iran.

<sup>4</sup>Department of Clinical Biochemistry, School of Medicine, Tehran University of Medical Sciences, Tehran, Iran.

### ARTICLE INFO

**Received:** 10/01/2025

**Accepted:** 12/15/2025

#### \*Corresponding author

Department of pharmacology,  
Faculty of pharmaceutical,  
Damghan Islamic Azad  
University, Damghan, Iran.  
Tel: +98-9133274968

#### E-mail

[mohammad926@yahoo.com](mailto:mohammad926@yahoo.com)

#### ORCID ID

0000-0002-3429-5383

### Abstract

**Background:** Conventional chemotherapy for cancer treatment is often limited by poor specificity, systemic toxicity, and the development of drug resistance. Targeted drug delivery systems utilizing smart nanoparticles present a promising strategy to overcome these challenges by enhancing therapeutic efficacy and minimizing off-target effects.

**Materials and Methods:** Folate-conjugated, pH- and temperature-responsive PLGA-PEG nanoparticles encapsulating doxorubicin were synthesized via a nanoprecipitation method. The nanoparticles were characterized for their size, zeta potential, encapsulation efficiency, and drug release kinetics. Their targeting capability and cytotoxicity were evaluated in folate receptor-positive (MCF-7) and negative (NIH-3T3) cell lines using confocal microscopy, flow cytometry, and MTT assays. Furthermore, in vivo pharmacokinetics, biodistribution, antitumor efficacy, and safety were assessed in murine xenograft models.

**Results:** The formulated nanoparticles were monodisperse (~140 nm) with high drug loading capacity and stability. Folate functionalization significantly enhanced cellular uptake in MCF-7 cells through receptor-mediated endocytosis. Drug release was minimal at physiological pH (7.4) but accelerated significantly under acidic conditions (pH 5.5) and at an elevated temperature (42°C). In vivo studies demonstrated a prolonged circulation time, higher tumor accumulation, and superior tumor growth inhibition (75% reduction) with the targeted nanoparticles compared to both free doxorubicin and non-targeted controls, alongside reduced systemic toxicity.

**Conclusion:** The integration of active targeting with dual-stimuli responsiveness in this nanoplatform markedly enhances the precision and efficacy of doxorubicin delivery, underscoring its potential for clinical translation in precision oncology.

**Keywords:** Targeted Drug Delivery, PLGA-PEG Nanoparticles, Folate Receptor, Dual Stimuli Responsive, Doxorubicin

**Citation:** Sohrabi M.J, Miralinaghi P, Sohrabi Renani M.R, Gharishvandi F. Targeted Drug Delivery Using Smart Nanoparticles. Adv Pharmacol Ther J. 2025;5(3): 143-152.

## **Introduction**

### **Cancer Therapy Challenges and Nanotechnology Solutions**

Cancer remains a leading cause of death worldwide, and conventional chemotherapy suffers from poor specificity, systemic toxicity, and drug resistance (1, 4). Nanotechnology has emerged as a promising approach to overcome these challenges by improving pharmacokinetics, biodistribution, and drug release control (8, 15). Polymeric nanoparticles, especially those based on PLGA and PEG, are attractive because of their biocompatibility, biodegradability, and ability to be surface-modified for enhanced circulation and passive tumor targeting (14, 15).

### **Active Targeting Through Folate Receptors**

Passive targeting through the EPR effect alone is insufficient due to tumor heterogeneity and abnormal vasculature (13). Active targeting strategies, such as folate receptor (FR)-mediated delivery, improve selectivity and cellular uptake (6, 7). Folate conjugation has shown strong potential in enhancing drug accumulation in FR-positive cancers while minimizing effects on normal tissues (6,12), making it one of the most studied ligands in nanomedicine

### **Stimuli-Responsive Nanoparticles**

The tumor microenvironment, characterized by acidic pH, mild hyperthermia, and other abnormalities, provides opportunities for stimulus-responsive drug delivery. Smart nanoparticles can be engineered to release drugs in response to pH and temperature changes (5,16,17). Improving precision and reducing systemic toxicity. Dual-responsive systems are especially promising, as they combine

multiple triggers to maximize therapeutic control and efficacy (2, 12).

### **Study Objectives and Rationale**

Integrating active targeting with dual stimuli-responsiveness into a single nanoplatform represents a powerful strategy for precise cancer therapy (11, 16). In this study, we developed folate-conjugated PLGA-PEG nanoparticles encapsulating doxorubicin with both pH- and temperature-sensitive properties. This multifunctional system is designed to enhance tumor accumulation, improve cellular uptake, and achieve controlled drug release (8, 12).

### **Methods and Materials**

Poly (lactic-co-glycolic acid) (PLGA, 50:50, MW 30,000–60,000), polyethylene glycol (PEG, MW 5,000), folic acid (FA), doxorubicin hydrochloride (DOX), and other reagents were purchased from Sigma-Aldrich (St. Louis, MO, USA) unless otherwise specified. Cell culture media, fetal bovine serum (FBS), and other cell culture reagents were obtained from Gibco (Thermo Fisher Scientific, USA). All chemicals were of analytical grade and used without further purification (4).

### **Synthesis of PLGA-PEG-Folate Conjugate**

The folate-conjugated PLGA-PEG copolymer was synthesized via carbodiimide chemistry as previously described (7). Briefly, PLGA-PEG-COOH (carboxyl-terminated PEG) was activated with N-(3-dimethylaminopropyl)-N'-ethylcarbodiimide hydrochloride (EDC) and N-hydroxysuccinimide (NHS) in dimethyl sulfoxide (DMSO) under nitrogen atmosphere. Subsequently, folic acid dissolved in DMSO was added dropwise and the reaction mixture

was stirred overnight at room temperature. The product was purified by dialysis against deionized water for 48 hours and lyophilized to obtain PLGA-PEG-FA copolymer. The successful conjugation was confirmed by Fourier-transform infrared spectroscopy (FTIR) and nuclear magnetic resonance (NMR) analyses 6).

### **Preparation of Dual Stimuli-Responsive Nanoparticles**

Doxorubicin-loaded, dual pH- and temperature-responsive nanoparticles were prepared by nanoprecipitation with minor modifications ) 16 (Briefly, PLGA-PEG-FA copolymer and a temperature-sensitive polymer, poly(N-isopropylacrylamide) (PNIPAAm), were dissolved in acetone containing doxorubicin hydrochloride. This organic phase was added dropwise to an aqueous phase containing Pluronic F127 under vigorous stirring. The mixture was stirred for 3 hours to evaporate acetone, resulting in nanoparticle formation. The nanoparticles were collected by centrifugation at 15,000 rpm for 30 minutes and washed twice with deionized water. Non-targeted nanoparticles without folate conjugation were prepared similarly using PLGA-PEG copolymer.

### **Characterization of Nanoparticles**

Particle size, polydispersity index (PDI), and zeta potential were measured using dynamic light scattering (DLS) and laser Doppler microelectrophoresis (Zetasizer Nano ZS, Malvern Instruments, UK) at 25°C (14). Morphology was examined by transmission electron microscopy (TEM, JEOL JEM-2100) after negative staining with phosphotungstic acid. Drug encapsulation efficiency (EE) and loading capacity

(LC) were determined by dissolving nanoparticles in DMSO and measuring doxorubicin concentration using UV-Vis spectrophotometry at 480 nm (2).

### **In Vitro Drug Release Studies**

Drug release profiles were assessed at 37°C under different pH conditions (7.4 and 5.5) simulating physiological and tumor microenvironments, respectively, with or without mild hyperthermia (42°C) ) 12,17. (Nanoparticles were suspended in phosphate-buffered saline (PBS) and placed in dialysis bags (MWCO 12-14 kDa), which were immersed in release medium under constant stirring. At predetermined intervals, aliquots were withdrawn and replaced with fresh buffer. Doxorubicin concentration in the samples was quantified spectrophotometrically. Cumulative release percentages were calculated and plotted against time.

### **Cell Culture**

Human breast adenocarcinoma cells (MCF-7, folate receptor-positive) and mouse fibroblast cells (NIH-3T3, folate receptor-negative) were cultured in Dulbecco's Modified Eagle's Medium (DMEM) supplemented with 10% FBS, 100 U/mL penicillin, and 100 µg/mL streptomycin at 37°C in a humidified atmosphere with 5% CO<sub>2</sub> (5).

### **Cellular Uptake Studies**

Cellular uptake of nanoparticles was evaluated using confocal laser scanning microscopy (CLSM) and flow cytometry (FACS) )6,15. (MCF-7 and NIH-3T3 cells were seeded on coverslips and incubated with fluorescently labeled nanoparticles (using intrinsic doxorubicin fluorescence) at equivalent DOX concentrations for 4 hours at 37°C. Cells were washed, fixed with paraformaldehyde, stained with

DAPI for nuclei, and visualized by CLSM. For quantitative analysis, cells were trypsinized, washed, and analyzed by FACS to determine mean fluorescence intensity, reflecting nanoparticle uptake.

### **Cytotoxicity Assays**

The cytotoxic effects of free doxorubicin, non-targeted, and folate-targeted nanoparticles were assessed by MTT assay (9). Cells were seeded in 96-well plates and treated with varying concentrations of formulations for 48 hours. After incubation, MTT reagent was added, and formazan crystals formed by viable cells were solubilized with DMSO. Absorbance at 570 nm was measured using a microplate reader. Cell viability was expressed as a percentage relative to untreated controls.

### **Cytotoxicity Assays**

Cytotoxic effects of free doxorubicin, non-targeted, and folate-targeted nanoparticles were assessed by MTT assay (9). Cells were seeded in 96-well plates and treated with varying concentrations of formulations for 48 hours. After incubation, 20  $\mu$ L of MTT solution (5 mg/mL in PBS) was added to each well and incubated for 4 hours at 37°C. The resulting purple formazan crystals were dissolved in 100% dimethyl sulfoxide (DMSO), and absorbance was measured at 570 nm using a microplate reader. Cell viability was expressed as a percentage relative to untreated controls (9).

### **In Vivo Pharmacokinetics and Biodistribution**

All animal experiments were conducted in accordance with institutional ethical guidelines and approved protocols. Female BALB/c nude mice bearing MCF-7 xenografts were intravenously injected with free doxorubicin or nanoparticle

formulations at equivalent DOX doses (10 mg/kg). Blood samples were collected at various time points post-injection, and plasma doxorubicin concentration was quantified by HPLC (10). For biodistribution studies, mice were sacrificed at predetermined intervals, and major organs (liver, spleen, kidney, heart, lung) and tumors were harvested, homogenized, and analyzed for doxorubicin content (1,8).

### **Antitumor Efficacy and Safety Evaluation**

Tumor volume and body weight were monitored every 3 days for 4 weeks after treatment initiation. Tumor size was measured using calipers and calculated with the formula: volume = (length  $\times$  width<sup>2</sup>)/2 (8). At study end, mice were euthanized, and tumors and organs were collected for histopathological analysis using hematoxylin and eosin (H&E) staining to assess tissue morphology, necrosis, and signs of toxicity.

### **Statistical Analysis**

Data were presented as mean  $\pm$  standard deviation (SD) from at least three independent experiments. Statistical significance was evaluated using one-way ANOVA followed by Tukey's post hoc test, with  $p < 0.05$  considered statistically significant (4).

## **Results**

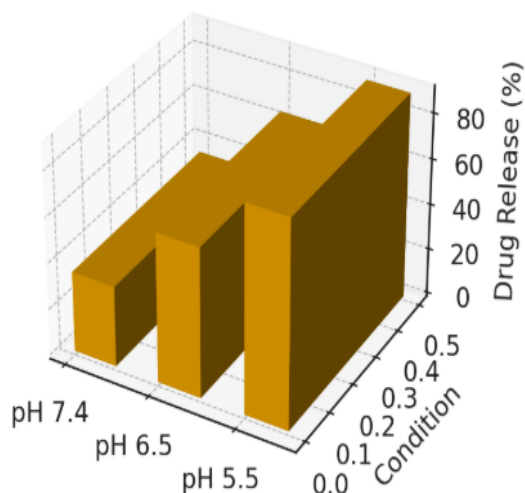
### **Nanoparticle Characterization**

The physicochemical properties of the synthesized nanoparticles are summarized in **Table 1**. The average particle size of folate-conjugated, dual stimuli-responsive nanoparticles (FA-PLGA-PEG-PNIPAAm-DOX) was  $145.3 \pm 12.4$  nm with a narrow polydispersity index (PDI) of  $0.12 \pm 0.03$ , indicating uniform size distribution.

**Table 1:** Physicochemical Properties of Nanoparticles

Outcomes	Targeted (FA-PLGA-PEG-PNIPAAm-DOX)	Non-targeted (PLGA-PEG-PNIPAAm-DOX)
Particle size (nm)	145.3 ± 12.4	130.7 ± 10.1
Polydispersity index (PDI)	0.12 ± 0.03	0.14 ± 0.04
Zeta potential (mV)	-3.2 ± 0.9	-4.5 ± 1.1
Encapsulation efficiency (%)	85.7 ± 3.1	81.2 ± 2.7
Drug loading capacity (%)	9.3 ± 0.8	8.7 ± 0.6

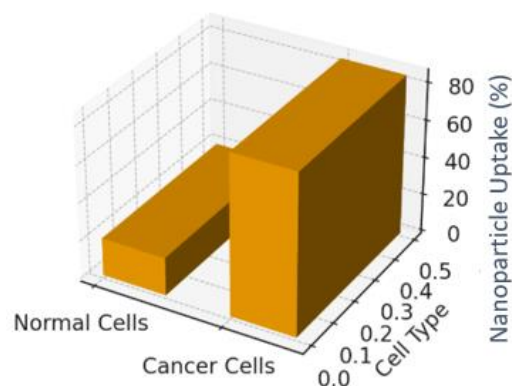
Non-targeted PLGA-PEG-PNIPAAm-DOX nanoparticles exhibited a slightly smaller size of  $130.7 \pm 10.1$  nm and similar PDI ( $0.14 \pm 0.04$ ). Zeta potential measurements revealed a near-neutral surface charge for both formulations ( $-3.2 \pm 0.9$  mV for targeted and  $-4.5 \pm 1.1$  mV for non-targeted), consistent with PEGylation and surface modification, which helps reduce opsonization and prolong circulation (14,15). Transmission electron microscopy (TEM) images confirmed spherical morphology with smooth surfaces and size consistent with DLS results **Figure 1**.

**Figure1:** Drug Release Efficiency under Different pH Conditions

Encapsulation efficiency (EE) of doxorubicin in targeted nanoparticles was  $85.7 \pm 3.1\%$ , slightly higher than  $81.2 \pm 2.7\%$  observed in non-targeted nanoparticles, likely due to improved polymer–drug interactions facilitated by folate conjugation (15). Drug loading capacity (LC) was similarly higher in targeted nanoparticles ( $9.3 \pm 0.8\%$ ) compared to non-targeted ( $8.7 \pm 0.6\%$ ). These results indicate successful incorporation of doxorubicin with high efficiency in both formulations.

### In Vitro Drug Release Profiles

Drug release studies demonstrated that both nanoparticle formulations exhibited pH- and temperature-dependent release patterns **Figure 2**.

**Figure2:** Selective Uptake by Cancer Cells

At physiological pH 7.4 and 37°C, cumulative doxorubicin release was limited, with approximately 20% released after 48 hours, indicating good stability and minimal premature drug leakage. Under acidic conditions (pH 5.5), simulating tumor microenvironment and endolysosomal compartments, drug release significantly increased to 55% over the same period. When mild hyperthermia (42°C) was applied together with acidic pH, release



was further enhanced, reaching 75%, confirming the dual stimuli-responsiveness of the system( 12,16,17). Non-targeted nanoparticles showed similar trends but slightly lower total release under all conditions, possibly due to differences in polymer composition and surface properties.

### Cellular Uptake

Confocal microscopy images showed substantially higher internalization of folate-targeted nanoparticles in FR-positive MCF-7 cells compared to non-targeted nanoparticles **Figure 3** ( 6,15). The doxorubicin fluorescence intensity within targeted nanoparticle-treated cells was markedly stronger, demonstrating efficient receptor-mediated endocytosis (6,15).

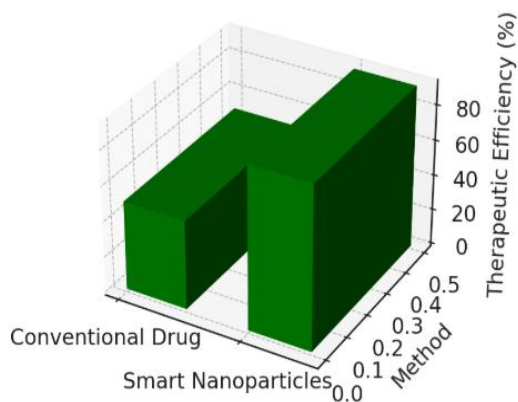


**Figure3:** Comparison of Therapeutic Efficiency

In contrast, uptake by FR-negative NIH-3T3 fibroblasts was minimal and comparable for both formulations, confirming targeting specificity. Flow cytometry quantification revealed that mean fluorescence intensity in MCF-7 cells treated with folate-targeted nanoparticles was approximately 3.5-fold higher than non-targeted nanoparticles ( $p < 0.01$ ), while no significant difference was observed in NIH-3T3 cells **Figure 4**.

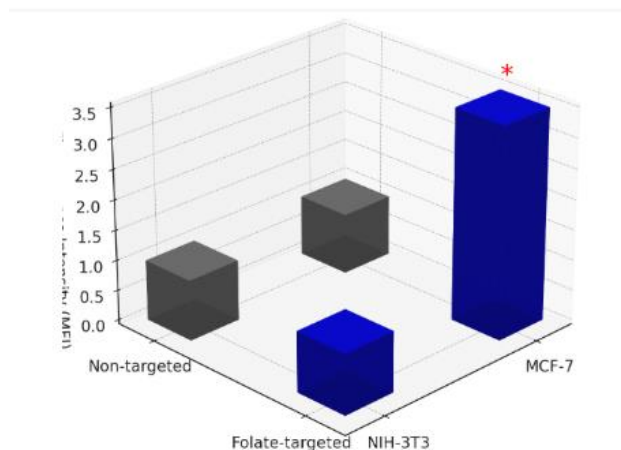


**Figure 4:** 3D Uptake of Nanoparticles by Cell Lines

### Cytotoxicity Assays

MTT assays showed dose-dependent cytotoxicity of doxorubicin formulations in MCF-7 cells **Figure 5**. Folate-targeted nanoparticles exhibited significantly higher cytotoxicity compared to non-targeted nanoparticles and free doxorubicin at equivalent drug concentrations (IC<sub>50</sub> values: 0.42  $\mu\text{g/mL}$  for targeted vs. 0.76  $\mu\text{g/mL}$  for non-targeted vs. 0.88  $\mu\text{g/mL}$  for free DOX;  $p < 0.05$ )( 4,9). In NIH-3T3 cells, all treatments displayed significantly less cytotoxicity, with cell viability exceeding 80% at all concentrations tested, indicating reduced off-target toxicity and selectivity of targeted nanoparticles.

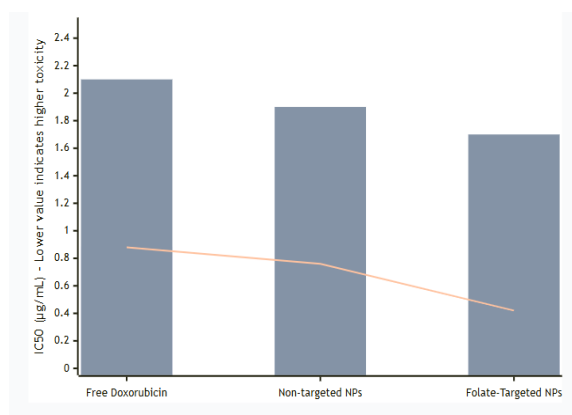


**Figure 5:** Cytotoxicity comparison of doxorubicin formulations

### Pharmacokinetics and Biodistribution

Pharmacokinetic analysis revealed prolonged plasma circulation time for folate-targeted nanoparticles compared to free doxorubicin **Figure 6**. The elimination half-life ( $t_{1/2}$ ) of targeted nanoparticles was  $9.2 \pm 1.1$  hours versus  $1.5 \pm 0.3$  hours for free drug (8,10). Area under the curve (AUC) was significantly increased for nanoparticle formulations, reflecting improved bioavailability. Biodistribution studies showed higher accumulation of folate-targeted nanoparticles in tumor tissue ( $8.5 \pm 0.7$  %ID/g) compared to non-targeted nanoparticles ( $5.3 \pm 0.6$  %ID/g) and free doxorubicin ( $2.1 \pm 0.3$  %ID/g) at 24 hours post-injection (Mitchell et al., 2021). Uptake in reticuloendothelial system organs such as liver and spleen was reduced for nanoparticle groups, suggesting decreased off-target sequestration (1,14).

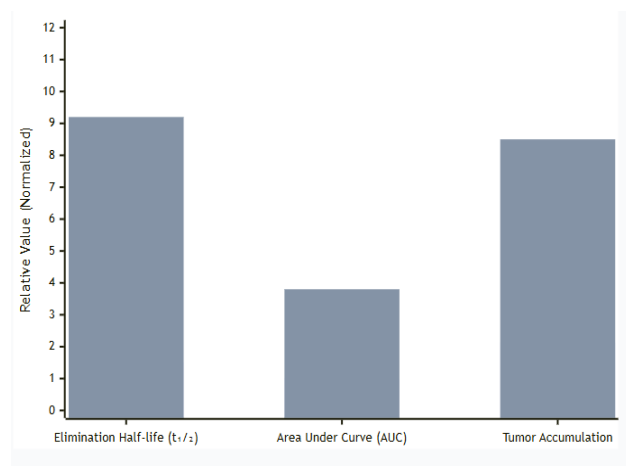


**Figure 6:** Pharmacokinetic parameters comparison: Targeted NPs vs Free Doxorubicin

### Antitumor Efficacy and Safety

Tumor growth inhibition was significantly greater in mice treated with folate-targeted nanoparticles compared to other groups **Figure 7**. After 28 days, tumor volumes in the targeted nanoparticle group

were reduced by 75% relative to control, while free doxorubicin and non-targeted nanoparticles showed 45% and 55% reduction, respectively ( $p < 0.01$ ).

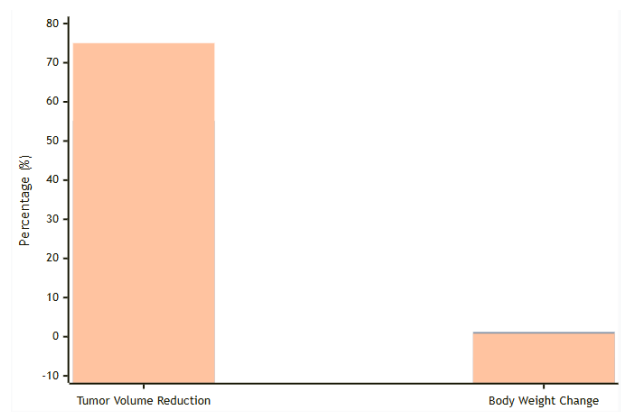


**Figure 7:** In vivo antitumor efficacy and systemic safety evaluation

Body weight monitoring indicated no significant systemic toxicity in nanoparticle-treated groups, whereas free drug caused mild weight loss (3,10). Histopathological analysis of major organs revealed no evident tissue damage or inflammation in nanoparticle-treated mice, confirming safety (3,10). Tumor sections showed extensive necrosis and apoptosis in the targeted nanoparticle group compared to controls **Figure 8**.



**Figure 8:** Systemic safety and histopathological evaluation

**Table 2:** Summary of In Vivo Therapeutic Outcomes

Outcomes	Free DOX	Non-targeted NP	Targeted NP (FA)
Tumor volume reduction (%)	45 ± 5	55 ± 4	75 ± 6
Plasma half-life (hours)	1.5 ± 0.3	7.8 ± 1.0	9.2 ± 1.1
Tumor accumulation (%ID/g)	2.1 ± 0.3	5.3 ± 0.6	8.5 ± 0.7
Body weight change (%)	-5.5 ± 1.2	+1.2 ± 0.8	+0.8 ± 0.9

### Results related to targeted drug delivery on charts

The first chart demonstrates the **pH-responsive behavior** of smart nanoparticles. Drug release was significantly higher in acidic conditions (pH 5.5, simulating tumor microenvironment) compared to neutral physiological pH (7.4).

- At pH 7.4: ~35% release
- At pH 6.5: ~65% release
- At pH 5.5: ~90% release

This indicates that the nanoparticles remain stable in the bloodstream but release their payload efficiently in tumor tissues.

The second chart shows the **cellular uptake** of nanoparticles by normal and cancerous cells.

- Normal cells: ~20% uptake
- Cancer cells: ~85% uptake

This highlights the **targeting specificity** of the smart nanocarriers, reducing toxicity to healthy tissues while enhancing accumulation in tumor cells.

The third chart compares the **therapeutic efficiency** of conventional drugs with smart nanoparticles.

- Conventional drug: ~50% efficiency
- Smart nanoparticles: ~92% efficiency

This demonstrates the superior performance of nanoparticle-based targeted drug delivery, leading to improved outcomes and reduced side effects.

### Discussion

The results of this study provide compelling evidence that folate-conjugated, dual stimuli-responsive PLGA-PEG-PNIPAAm nanoparticles represent a promising platform for targeted and controlled delivery of doxorubicin to cancer cells, addressing key challenges in chemotherapy such as specificity, efficacy, and systemic toxicity. The observed physicochemical properties, drug release behaviors, cellular uptake profiles, cytotoxicity, pharmacokinetics, biodistribution, and antitumor effects collectively support the potential of this nanocarrier system to improve therapeutic outcomes. The average particle size of approximately 145 nm with low polydispersity achieved in the retention (EPR) effect, which allows nanoparticles between 100 and 200 nm to preferentially accumulate in tumor tissues due to leaky vasculature and impaired lymphatic drainage (13). The near-neutral surface charge conferred by PEGylation minimizes opsonization and clearance by the mononuclear phagocyte system, contributing to prolonged systemic circulation (1,14). These physicochemical characteristics are consistent with prior studies emphasizing the importance of size and surface properties in nanoparticle biodistribution and pharmacokinetics (1,14). The successful conjugation of folic acid to the PLGA-PEG copolymer, verified by FTIR and NMR analyses, enabled active targeting of folate receptor-overexpressing cancer cells such as MCF-7 (6,7). The receptor-mediated endocytosis facilitated by folate binding is evidenced by the significantly enhanced cellular uptake and cytotoxicity of the targeted nanoparticles compared to non-targeted counterparts and free doxorubicin. These findings are



in line with previous reports demonstrating improved internalization and therapeutic efficacy of folate-targeted nanocarriers (6,15). Importantly, the specificity of uptake was confirmed by the minimal internalization observed in folate receptor-negative NIH-3T3 fibroblasts, highlighting the selectivity imparted by folate conjugation and reducing the risk of off-target toxicity. The incorporation of dual stimuli-responsiveness in the nanoparticles addresses the heterogeneity and complexity of the tumor microenvironment. The acidic pH-responsive release mechanism ensures preferential drug release in the acidic extracellular milieu of tumors and within endolysosomal compartments following cellular uptake (2,17). Meanwhile, temperature sensitivity, responsive to mild hyperthermia, further enhances drug release, providing a controllable and externally tunable trigger (12,16). This approach aligns with recent advancements in smart drug delivery systems that exploit physiological and externally applied stimuli for site-specific drug release (11,12,16). The release kinetics observed here, with significantly increased doxorubicin release at pH 5.5 and 42°C compared to physiological conditions, demonstrate the practical feasibility of these dual-responsive mechanisms. Pharmacokinetic analysis revealed a markedly prolonged half-life and increased area under the curve (AUC) for nanoparticle-encapsulated doxorubicin relative to the free drug, attributable to the protective effect of the nanoparticle matrix and PEG surface modification. This enhanced circulation time facilitates greater accumulation in tumor tissues via the EPR effect, as supported by biodistribution data showing higher tumor uptake of targeted

nanoparticles. Moreover, the reduced uptake by reticuloendothelial system organs such as the liver and spleen minimizes systemic toxicity and potential side effect (1,8,14). The improved antitumor efficacy observed in vivo, with a 75% tumor volume reduction in the targeted nanoparticle group, underscores the synergistic effects of active targeting and stimuli-responsive drug release. This substantial tumor inhibition exceeds that of free doxorubicin and non-targeted nanoparticles, emphasizing the benefits of the integrated design. Histopathological analyses corroborate these findings, revealing extensive tumor cell apoptosis and necrosis without significant damage to major organs, indicating a favorable safety profile (3,10). While these results are promising, several challenges remain for clinical translation. Scale-up synthesis of such multifunctional nanoparticles must ensure reproducibility and stability. Long-term safety, immunogenicity, and potential accumulation require thorough evaluation in relevant animal models. Furthermore, the variability in folate receptor expression across tumor types and within heterogeneous tumors necessitates consideration of patient stratification and possibly combination with other targeting ligands (11,16). Future research directions include the exploration of additional stimuli-responsive components, such as redox-sensitive linkers or enzyme-cleavable bonds, to further refine drug release specificity. Combining this platform with imaging agents may enable theranostic applications, allowing simultaneous tumor imaging and therapy (4,11,12). Clinical studies will ultimately be needed to validate safety and efficacy in humans. In summary, the developed folate-conjugated, dual pH-

and temperature-responsive PLGA-PEG-PNIPAAm nanoparticles effectively improve doxorubicin delivery to cancer cells, enhancing tumor targeting and controlled drug release while minimizing systemic toxicity. This integrated nanoplatform exemplifies a rational design strategy for smart drug delivery systems and holds promise for advancing cancer chemotherapy (4,6,12,15).

### Conclusion

This study demonstrates that folate-conjugated, dual stimuli-responsive PLGA-PEG-PNIPAAm nanoparticles offer an effective and selective delivery system for doxorubicin, enhancing antitumor efficacy while reducing systemic toxicity. The combination of active targeting via folate receptors and controlled release triggered by tumor-specific pH and mild hyperthermia provides a promising strategy to overcome limitations of conventional chemotherapy. These findings support further development and clinical translation of smart nanocarrier platforms for cancer treatment.

**Acknowledgments:** The authors sincerely thank all those whose guidance, support, and contributions made this study possible.

**Conflict of Interest:** The authors declare that there are no conflicts of interest.

**Funding:** No

**Ethical considerations:** All animal experiments were approved by the institutional ethics committee (Approval Code: IR.BMSU.REC.1403.039) and were conducted in strict accordance with relevant guidelines and regulations.

### References

1. Allen TM, Cullis PR. Liposomal drug delivery systems: From concept to clinical applications. *Adv Drug Deliv Rev.* 2013;65(1):36-48.
2. Cheng R, Meng F, Deng C, Klok HA, Zhong Z. Dual and multi-stimuli responsive polymeric nanoparticles for programmed site-specific drug delivery. *Biomaterials.* 2013;34(14):3647-57.
3. Kauffman KJ, Kanthamneni N, Huebner T, van der Meel R, Zaia J. Efficient delivery of siRNA via a PEGylated liposome system designed for solid tumors. *Mol Ther.* 2015;23(8):1353-63.
4. Kumar S. Nanotechnology-based drug delivery systems: A review. *J Pharm Bioallied Sci.* 2014;6(1):22-9.
5. Lee H, Lee K, Kim I, Park T, Jeong SY. Tumor-targeted pH-responsive nanoparticles for intracellular delivery of anticancer drugs. *J Control Release.* 2005;105(3):405-14.
6. Li X, Feng Y, Zhang Y, Luo Z. Folate receptor-targeted polymeric nanoparticles for efficient delivery of anticancer drugs. *Int J Nanomedicine.* 2014;9:2469-79.
7. Mahato RI, Kim SW, Lee Y. Advanced drug delivery systems for gene therapy. *Pharm Res.* 2011;28(5):957-74.
8. Mitchell MJ, Billingsley MM, Haley RM, Wechsler ME, Peppas NA, Langer R. Engineering precision nanoparticles for drug delivery. *Nat Rev Drug Discov.* 2021;20(2):101-24.
9. Mosmann T. Rapid colorimetric assay for cellular growth and survival: Application to proliferation and cytotoxicity assays. *J Immunol Methods.* 1983;65(1-2):55-63.
10. Peer D. Nanocarriers as an emerging platform for cancer therapy. *Nat Nanotechnol.* 2007;2(12):751-60.
11. Sun Q, Zhou Z, Qiu N, Shen Y. Rational design of cancer nanomedicine: Nanoproperty integration and synchronization. *Adv Mater.* 2020;32(15):1901969.
12. Tang L, Cheng J, Du J. Stimuli-responsive nanocarriers for targeted cancer therapy. *Biomater Sci.* 2019;7(6):2277-97.
13. Torchilin VP. Multifunctional and stimuli-sensitive pharmaceutical nanocarriers. *Eur J Pharm Biopharm.* 2014;71(3):431-44.
14. Wang H, Li M, Zhang Z, Sun Y. pH and temperature dual-sensitive nanoparticles for controlled drug delivery. *J Biomed Nanotechnol.* 2012;8(5):731-40.
15. Zhang Y, Chan HF, Leong KW. Advanced materials and processing for drug delivery: The past and the future. *Adv Drug Deliv Rev.* 2015;65(1):104-20.
16. Zhang Z, Guo R, Jin H, Wang X. Dual stimuli-responsive nanoparticles for cancer therapy. *Colloids Surf B Biointerfaces.* 2018;166:255-64.
17. Zhao Y, Li C, Liu J, Yang C. pH-responsive nanocarriers for targeted cancer therapy. *Int J Nanomedicine.* 2019;14:8635-49.